Evolutionary Ecology Research, 2006, **8**: 591–604

Population dynamics of Batesian mimicry under interspecific competition

Fuga Kumazawa,[1,2] Takahiro Asami,[2]* Tarou Hayashi[1] and Jin Yoshimura[1,3,4]

[1]*Department of Systems Engineering, Shizuoka University, Hamamatsu 432-8561, Japan,*
[2]*Department of Biology, Shinshu University, Matsumoto 390-8621, Japan,*
[3]*Marine Biosystems Research Centre, Chiba University, Kamogawa 299-5502, Japan*
and [4]*Department of Environmental and Forest Biology, State University of New York, College of Environmental Science and Forestry, Syracuse, NY 13210, USA*

ABSTRACT

Question: What is the basic feature of population dynamics of Batesian mimicry under interspecific competition?

Mathematical method: We built the population dynamics equation of Batesian mimicry under Lotka-Volterra competition. By means of the phase plane analysis, we examine the dynamics and equilibria in comparison with the four unique phase planes of the Lotka-Volterra competition model with no mimicry.

Key assumptions: Both the benefit of mimicry for a palatable species mimicking a distasteful model species and the cost for the model are dependent on their frequencies relative to each other. The mortality of the model by predation increases as the frequency of the mimic increases, while the mortality of the mimic decreases as the frequency of the model increases.

Predictions: The mimetic species in general benefits from mimicry depending on the adult predatory mortality. The assemblage of the model and mimetic species reaches different equilibria depending on whether the benefit of the mimic or the cost of the model increases under interspecific competition. The most complicated phase plane appears between stable co-existence of the assemblage and survival of the mimetic species only, depending on the initial conditions.

Conclusion: The benefit of the mimic and the cost of the model are key factors in determining the evolutionary process of Batesian mimicry.

Keywords: Batesian mimicry, frequency dependence, Lotka-Volterra competition, predation.

INTRODUCTION

Batesian mimicry is one of the most powerful ways of demonstrating the outcome of adaptive evolution by natural selection in the wild (Fisher, 1930; Sheppard, 1958; Ford, 1975; Turner, 1977). It is known in a wide range of both animals and plants (Wickler, 1968). In Batesian mimicry, a palatable species resembles the conspicuous appearance of a sympatric model species that

* Author to whom all correspondence should be addressed. e-mail: asami99@shinshu-u.ac.jp

is protected from predation. When the naive predator attacks the model, it learns the model appearance through noxious experience with the model. The predator then avoids attacking prey candidates that have a similar appearance to the model. Thus the palatable mimics gain a benefit of reduced predation risk in sympatry (Bates, 1862).

Several studies have employed mathematical models to explore the evolutionary dynamics of predator–prey interactions with mimicry (Huheey, 1964; Emlen, 1968; Estabrook and Jesperson, 1974; Luedeman *et al.*, 1981; Turner *et al.*, 1984; Turner and Speed, 1996; Speed and Turner, 1999; Speed, 2001; Johnstone, 2002; Sasaki *et al.*, 2002; Sherratt, 2002, 2003; Kokko *et al.*, 2003; Franks and Noble, 2004; Sherratt *et al.*, 2004). However, these models have only embedded or assumed the population dynamics of mimicry to investigate evolutionary processes in a species assemblage of the model and mimic, and have not explicitly examined the population dynamics of Batesian mimicry.

Yamauchi (1993) has constructed a mathematical model to demonstrate the dynamics of Batesian model and mimetic populations, with no assumption of competition between the model and mimic. His model has successfully demonstrated multiple dynamic equilibria observed in the model and mimic in the wild. However, it was not capable of sustaining the model population in allopatry without the invasion of the mimic.

The model and mimic are likely to share common resources such as nectar in sympatry, although the two species may not be close in phylogeny. Thus, it would be reasonable to assume their competitive interactions. In the present study, we explored population dynamics in Batesian mimic and model species that compete for common resources in Lotka-Volterra competition.

In Batesian mimicry, an increase in the frequency of the mimic relative to the model increases the chance of predators learning the mimetic appearance as the searching image of palatable prey (Turner and Speed, 1996; Speed and Turner, 1999). It would then increase the mortality of both the model and mimic populations. Here we assume that the mortalities of the mimic and model are dependent on the frequency of competitive opponents. We analyse the equilibria using the phase planes, in comparison with those expected under Lotka-Volterra competition with no mimicry. We discuss the implications of the population dynamics elucidated for understanding the evolutionary process of Batesian mimicry.

MODEL CONSTRUCTION

General assumptions

Batesian mimicry involves animal species with three major roles: a protected model, a palatable mimic, and a predator. A naive predator that has no experience of the noxious model attacks it as prey. Because of noxious protection such as the model's distastefulness or toxicity, the naive predator learns the model's appearance to avoid attacking it, unless the naive predator lacks the ability to learn. Because of morphological or behavioural mimicry (e.g. Howarth *et al.*, 2004), predators that have experienced the noxious model also avoid the mimetic species. However, if the predator experiences palatable mimics, then the predator could learn their wing pattern or behaviour as the searching image of a suitable prey and start attacking both the mimic and model. Therefore, the mortality of the mimic and model species would be positively correlated with the frequency of the mimic in the assemblage of model and mimetic populations. For simplicity, we assumed that male and female mimics exhibit a common mimetic appearance or behaviour without non-mimetic morphs.

Population dynamics equation

Predatory mortality is built into population dynamics of Lotka-Volterra competition (Yoshimura and Clark, 1994). Here $B_i = B_i(N_i, N_j, \alpha_{ij})$ denotes the birth rate, and $M_i = M_i(N_i, N_j, \alpha_{ij})$ the death rate. The overall growth rate is $R_i = B_i - M_i$, which includes density dependence induced by interspecific competition. Then the population dynamics equation is expressed as

$$\frac{\mathrm{d}N_i}{\mathrm{d}t} = (B_i - M_i)N_i = R_i N_i \tag{1}$$

Death may or may not be caused by predators. By introducing the proportion of mortality that is induced by predation, p_i for $0 \le p_i \le 1$, we divide the mortality into predatory and non-predatory fractions, such that

$$\frac{\mathrm{d}N_i}{\mathrm{d}t} = \{B_i - (1 - p_i)M_i - p_i M_i\}N_i \tag{2}$$

where the terms B_i and M_i are defined as

$$B_i = b_{ik} + (b_{i0} - b_{ik})\left(1 - \frac{N_i + \alpha_{ij}N_j}{K_i}\right) \tag{3}$$

$$M_i = m_{i0} + (m_{ik} - m_{i0})\left(\frac{N_i + \alpha_{ij}N_j}{K_i}\right) \tag{4}$$

Here the terms b_{i0} and m_{i0} denote the intrinsic birth and death rates respectively, while the terms b_{ik} and m_{ik} denote the birth and death rates at the carrying capacity $N_i = K_i$ respectively. The term α_{ij} is the Lotka-Volterra competition coefficient of species j on species i. Note that $b_{ik} = m_{ik}$ because of the definition of carrying capacity where the birth rate is balanced with the mortality (Yoshimura and Clark, 1994). In equations (3) and (4), b_{ik} and m_{i0} are independent of density. In contrast, the second terms are density-dependent. Therefore, by definition of the birth and death rates, it should be satisfied that $b_{i0} - b_{ik} \ge 0$ and $m_{ik} - m_{i0} \ge 0$.

We should also note that the fraction p_i for $0 \le p_i \le 1$ is the mortality caused by predation in the adult stage. Here we assume that the same value of p_i is used for both mortality terms that are dependent and independent of density. However, the fraction p_i may be different between these two terms. In the extreme case, predatory mortality could be entirely density-dependent or density-independent. In the Discussion, we briefly show that the predicted outcome remains qualitatively similar.

The predatory mortality here is different from the usual functional responses in common prey–predator models. We suppose that the predator community is large and stable and does not depend on consumption of the model and mimetic individuals. When the prey density is higher, they have to spend more time exposed to predation, because they need to forage more in sites with higher predation risk after low-risk sites have been depleted. The predators may also focus on them as an easy and common food resource when their density is higher. Thus we assume that the predatory mortality depends on the prey density as in the usual Lotka-Volterra competition model.

Frequency dependence

Suppose two sympatric species S_i ($i = 1,2$), where $i = 1$ indicates the model and $i = 2$ the mimic. Mimicry changes the predation mortality. The effect of mimicry on the mortality depends on the frequency of competitors (d_i):

$$d_i = d(N_i, N_j) = N_j/(N_i + N_j) \tag{5}$$

where N_i and N_j are the population sizes of species i and species j respectively. We assume $N_i + N_j \geq 1$ and thus $d_i \geq 0$.

Introducing the effects of mimicry (equation 5) into the competition dynamics (equation 2), we get

$$\frac{dN_1}{dt} = \{B_1 - (1 - p_1)M_1 - (1 + d_1)p_1M_1\}N_1 = (R_1 - d_1p_1M_1)N_1 \tag{6}$$

$$\frac{dN_2}{dt} = \{B_2 - (1 - p_2)M_2 - (1 - d_2)p_2M_2\}N_2 = (R_2 + d_2p_2M_2)N_2 \tag{7}$$

Here the effect of mimicry is only expressed as predatory mortality (p_i). Furthermore, this effect is negative ($-d_1$) for the model species S_1 and positive ($+d_2$) for the mimic species S_2. Note that d_i becomes d_1 in equation (6) and d_2 in equation (7), because the effects of mimicry depend on the frequency of competitors.

The effects of frequency dependence d_i on the model may also be weaker than those on the mimic. For example, beak marks on butterfly wings indicate that they have escaped from a bird predator's attacks (e.g. Ohsaki, 1995). A predator that leaves a beak mark will have tasted a piece of fragile wing without killing the butterfly (DeVries, 2002). Thus, the model would have a better chance of surviving after the initial unsuccessful attack than the mimic that may be killed through immediate repeated attacks by the same predator, even when the model has become extremely rare ($d_1 = 1$ in equation 6). In contrast, the mimic escapes completely from attacks by predators when it is rare ($d_2 = 1$ in equation 7). We could include additional parameters in the current model to manipulate this asymmetry in the frequency dependence of predatory mortality between the model and mimic. However, to avoid further complexity with parameters already involved, we assume inherent inequality of their predatory mortalities, such as $p_1 < p_2$ and/or $M_1 < M_2$.

All phase planes were drawn directly by Mathematica (Wolfrum Research Inc.) with parameter values $b_{1k} = m_{1k} = 0.1$, $b_{2k} = m_{2k} = 0.2$, $b_{10} = 0.2$, $m_{10} = 0.09$, $b_{20} = 0.3$ and $m_{20} = 0.14$ unless otherwise specified.

RESULTS

Setting $dN_i/dt = 0$, we obtain the zero-growth isoclines for the model and mimic (Fig. 1). The isocline for the model is lower than the isocline of the Lotka-Volterra competition model with no mimicry (Fig. 1A). The N_2-intercept c_1 and N_1-intercept c_2 are given by

$$c_1 = \frac{b_{10} - (1 + p_1)m_{10}}{b_{10} - (1 + p_1)m_{10} + p_1b_{1k}} \frac{k_1}{\alpha_{12}} \tag{8}$$

$$c_2 = \frac{b_{20} - (1 - p_2)m_{20}}{b_{20} - (1 - p_2)m_{20} - p_2b_{2k}} \frac{k_2}{\alpha_{21}} \tag{9}$$

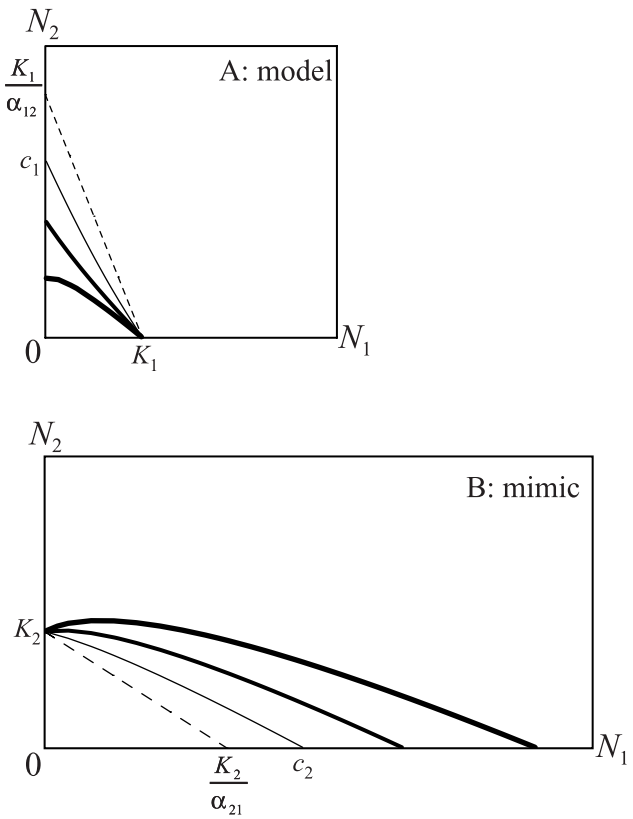

Fig. 1. The zero-growth isocline in population dynamics of frequency dependence (solid line). The predation fraction of mortality p_i is varied (thin line: $p_i = 0.3$; intermediate line: $p_i = 0.6$; thick line: $p_i = 0.9$). The isoclines of the Lotka-Volterra competition model with no mimicry are also shown for comparison (dotted line). (A) Model species. The N_2-intercept c_1 is smaller than K_1/α_{12} when mortality is positively frequency dependent. (B) Mimetic species. The N_1-intercept c_2 is larger than k_2/α_{21} under positive frequency dependence.

These intercepts are limited within a certain range. The range of the N_2-intercept c_1 is given by

$$\frac{K_1}{\alpha_{12}} \geq c_1 \geq \frac{2m_{10} - b_{10}}{2m_{10} - b_{10} - b_{1k}} \frac{K_1}{\alpha_{12}} \tag{10}$$

where the upper and lower bounds correspond to $0 \leq p_1 \leq 1$ respectively. On the other hand, the isocline for the mimic is higher than the isocline under Lotka-Volterra competition with no mimicry. The range of the N_1-intercept c_2 is given by

$$\frac{K_2}{\alpha_{21}} \leq c_2 \leq \frac{b_{20}}{b_{20} - b_{2k}} \frac{K_2}{\alpha_{21}} \tag{11}$$

where the lower and upper bounds correspond with $0 \leq p_2 \leq 1$ respectively.

The current mimicry model is expanded from the standard Lotka-Volterra equation ($p_1 = p_2 = 0$). As the p's increase in Fig. 1, there is an effect of the mimicry interaction which is beneficial to the mimic (its nullcline moves up in the (N_1, N_2) plane) and harmful to the model (its nullcline moves down). The possible effects of mimicry can therefore be expressed in terms of threshold values of the predatory portions of mortality p_1 and p_2 (see Appendix 1 for details). Below a threshold, the model acts like the corresponding Lotka-Volterra model without mimicry. Above a threshold, however, things can change generally to the benefits of the mimic.

Figures 2–5 show the phase planes of Batesian mimicry under Lotka-Volterra competition. Each figure corresponds to one of the four cases of the Lotka-Volterra phase plane. Figure 2A is the case where only S_1 survives in the Lotka-Volterra system ($K_1 > K_2/\alpha_{21}$ and $K_2 < K_1/\alpha_{12}$). S_1 survives as in the Lotka-Volterra system when $K_1/\alpha_{12} \geq c_1 > K_2$ and $K_2/\alpha_{21} \leq c_2 < K_1$; that is, $0 \leq p_1 < p_1^*$ and $0 \leq p_2 < p_2^*$ respectively, where the two thresholds p_1^* and p_2^* are defined as

$$p_1^* = \frac{(b_{10} - m_{10})(K_1 - \alpha_{12}K_2)}{m_{10}K_1 + (b_{1k} - m_{10})\alpha_{12}K_2} \tag{12}$$

$$p_2^* = \frac{(b_{20} - m_{20})(\alpha_{21}K_1 - K_2)}{m_{20}K_2 + (b_{2k} - m_{20})\alpha_{21}K_1} \tag{13}$$

The right-hand equality holds for either p_1^* or p_2^*, but not both (see below for when both hold). Similarly, the combinations of p_1 and p_2, instead of c_1 and c_2, can describe all other cases. Note that when $p_i = p_i^*$, $c_i = K_j$ for $i \neq j$. Thus p_1^* and p_2^* are the common thresholds for the current phase planes.

Figure 2B shows that the model (S_1) and mimic (S_2) co-exist, when $p_1 < p_1^*$ and $p_2 > p_2^*$. Figure 2C shows that either S_1 or S_2 survives, when $p_1 > p_1^*$ and $p_2 < p_2^*$. Figure 2D shows that only S_2 survives when $p_1 \gg p_1^*$ and $p_2 \gg p_2^*$. When the values of both p_i are slightly larger but close to p_i^*, depending on the curvature of both phase planes, there may be two stable equilibria and one unstable equilibrium (Fig. 2E). In this case, the co-existence of species S_1 and S_2 or the survival of S_2 alone is a possible outcome depending on the initial conditions. However, this seems to be rare under the combinations of possible parameter values. In Fig. 2F, $c_1 = K_2$ and $c_2 = K_1$ (i.e. $c_i = K_j$), which means $p_i = p_i^*$ for $i = 1$ and 2. In this case, a narrow crescent shape starting from $N_1 = K_1$ to $N_2 = K_2$ appears, where $N_1 = K_1$ is the only stable equilibrium and thus only S_1 survives as in Fig. 2A.

Figure 3 is the case where only S_2 survives in the Lotka-Volterra system ($K_1 < K_2/\alpha_{21}$ and $K_2 > K_1/\alpha_{12}$). Figure 4 shows the case where only either S_1 or S_2 survives in the Lotka-Volterra system ($K_1 > K_2/\alpha_{21}$ and $K_2 > K_1/\alpha_{12}$). Figure 4A shows that only either S_1 or S_2 persists when $p_2 < p_2^*$. Figure 4B shows that only S_2 survives when $p_2 \geq p_2^*$. Figure 5 is the case where both S_1 and S_2 persist in the Lotka-Volterra system ($K_1 < K_2/\alpha_{21}$ and $K_2 < K_1/\alpha_{12}$). Figure 5A shows that only S_2 survives when $p_1 \geq p_1^*$. Figure 5B shows that S_1 and S_2 co-exist when $p_1 < p_1^*$.

We also analysed the case with no competition – that is, $\alpha_{ij} = 0$ (dotted straight lines in Fig. 6). By introducing Batesian mimicry, the two species become dependent on each other. The stable equilibrium moves upward and leftward (Fig. 6A). When p_i is larger, it moves further (Fig. 6B).

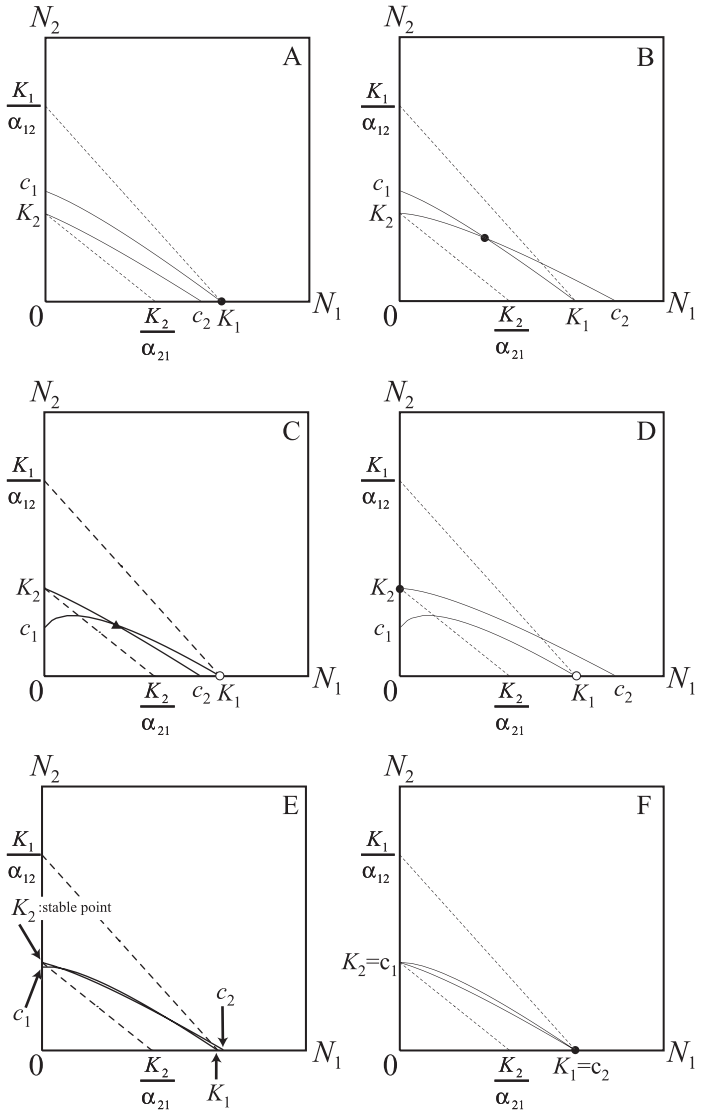

Fig. 2. Phase planes in population dynamics of Batesian mimicry when only the model species (S_1) survives under Lotka-Volterra competition. The isoclines are anchored at (K_1, 0) and (0, c_1) for the model, and at (0, K_2) and (c_2, 0) for the mimic (S_2). Solid circles and lines are for mimicry and open circles and dotted lines are for Lotka-Volterra competition with no mimicry. (A) No change in the equilibrium (S_1 only) is expected when $p_i \leq p_i^*$ for $i = 1$ and 2. (B) Stable co-existence (S_1 and S_2) is expected when $p_1 < p_1^*$ and $p_2 > p_2^*$. (C) Initial dependence (either S_1 or S_2) is expected when $p_1 > p_1^*$ and $p_2 < p_2^*$. The solid triangle indicates a saddle point. (D) Replacement (S_2 only) is expected when the proportions of predatory mortality in both species are sufficiently larger than the corresponding thresholds (i.e. $p_i \gg p_i^*$). (E) Complicated phase plane with either only S_2 or co-existence is expected when the proportions of predatory mortality are slightly larger than their thresholds (i.e. $p_i > p_i^*$ and $p_i \approx p_i^*$). There is one stable and one unstable equilibrium. (F) Similar to (A) but when $p_i = p_i^*$ for $i = 1$ and 2.

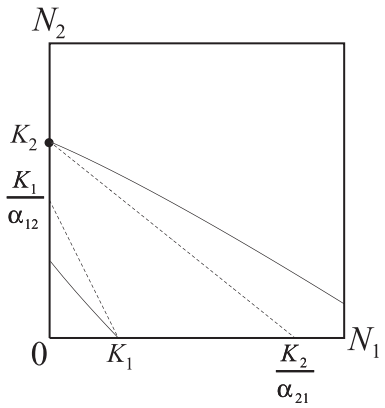

Fig. 3. Phase plane in population dynamics of Batesian mimicry when only the mimic (S_2) persists in Lotka-Volterra competition. The point of stable equilibrium is identical to that in the Lotka-Volterra system with no mimicry.

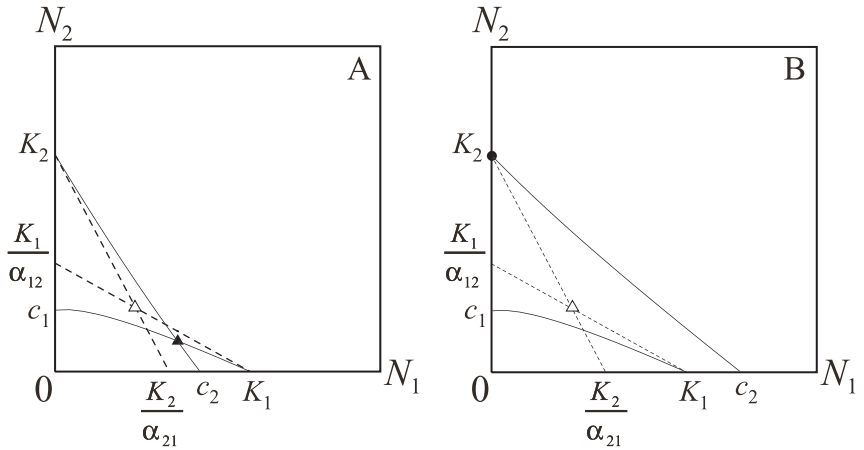

Fig. 4. Phase planes in population dynamics of Batesian mimicry when either the model (S_1) or mimic (S_2) survives in Lotka-Volterra competition (triangles indicate unstable equilibria, i.e. saddle points). (A) When $p_2 < p_2^*$, either S_1 or S_2 survives. The solid triangle is a saddle point. (B) When $p_2 \geq p_2^*$, only S_2 persists.

DISCUSSION

The present study has shown that density-dependent competition between the model and mimetic species leads their populations to diverse equilibria depending on the relative values of parameters. The results are strikingly different from those in the model of Yamauchi (1993), which includes no interspecific competition. As expected of mimicry, the benefit for the mimic population increases in all cases. However, some unexpected results were observed such that only the model persists under resource competition with the mimic. The mimic may co-exist with the model when the mimic gains a certain amount of benefit (Fig. 2B). In contrast, the model and mimic exclude each other depending on the condition if the

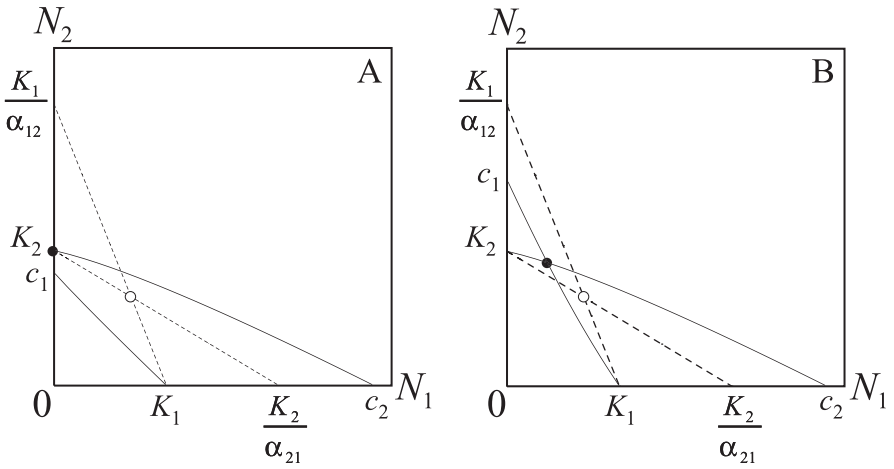

Fig. 5. Phase planes in population dynamics of Batesian mimicry when both the model (S_1) and mimic (S_2) co-exist in Lotka-Volterra competition (open circles: stable equilibria with no mimicry; solid circles: those with mimicry). (A) When $p_1 \geq p_1^*$, S_2 wins with mimicry. (B) When $p_1 < p_1^*$, S_1 and S_2 co-exist with mimicry.

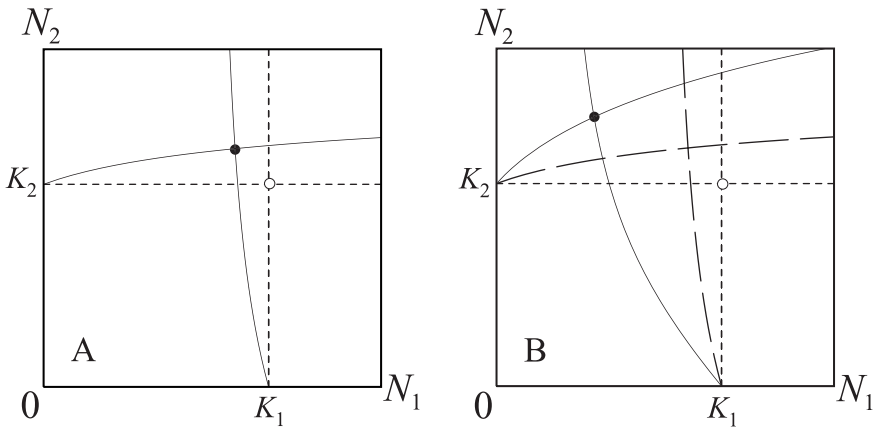

Fig. 6. Phase planes in population dynamics of Batesian mimicry without Lotka-Volterra competition (open circles: stable equilibria with no mimicry; solid circles: those with mimicry). Frequency-dependent mortality shifts the equilibrium densities of the model and mimic. (A) When p_i is small ($p_i = 0.3$). (B) When p_i is large ($p_i = 0.9$).

model gains no benefit (Fig. 2C). The mimic excludes the model if the mimic gains benefit to a certain extent while the model gains nothing (Fig. 2D). These results correspond with the four cases of Lotka-Volterra phase planes. Whether both species co-exist or only the mimic persists depends on the initial conditions, when the proportions of predatory mortality are approximately equal or slightly larger than the thresholds (Fig. 2E). This is the new phase plane that never appears in Lotka-Volterra competition with no mimicry.

In the present model, we assume that the effects of mimicry (p_i) are proportional to the overall adult predatory mortality. Thus these effects are equally distributed to both density-

dependent and density-independent mortalities. However, in extreme cases, these effects may be either dependent or independent of density. Figure 7 shows the phase planes in these extreme cases. When mimicry only affects the density-independent mortality (Figs. 7A and 7B), the effects are similar to those in the proportional case (Fig. 1). In contrast, when mimicry only affects the density-dependent mortality (Figs. 7C and 7D), the effects on the model species are minimized, whereas those on the mimic are similar to those in the proportional case (Fig. 1B). The N_1- and N_2-intercepts, c_1 and c_2 (see equations 8 and 9), for these cases and their corresponding thresholds, p_1* and p_2* (see equations 12 and 13), are listed in the Appendix. From the above graphical interpretation, the qualitative results appear to be similar to the current results. However, a full analysis will be required to verify them.

From the evolutionary perspective of mimicry, the model should be protected from predation by its own noxious traits and thus be sustained unless the cost of noxiousness

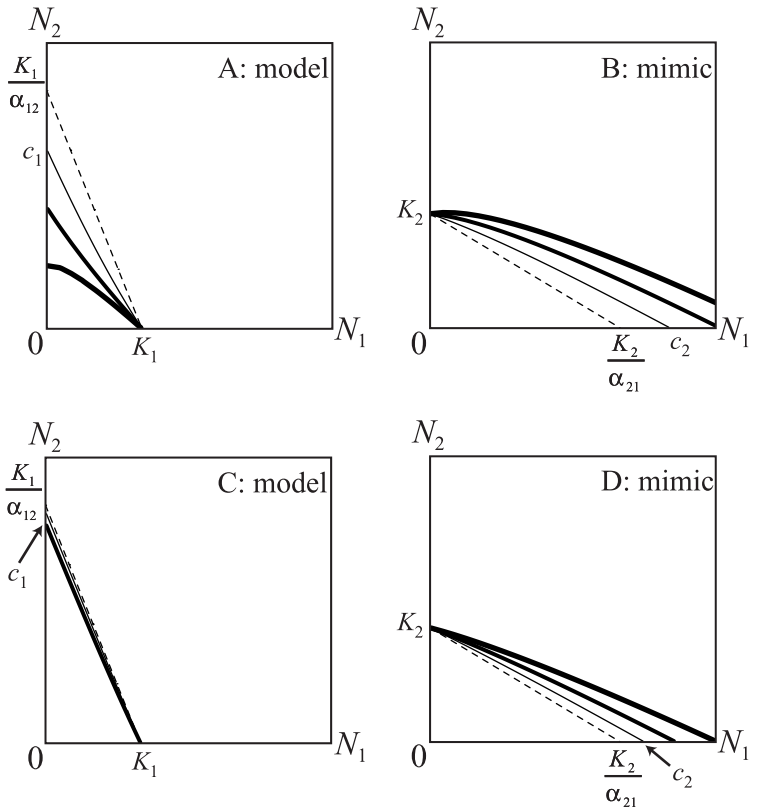

Fig. 7. The zero-growth isoclines in population dynamics of Batesian mimicry where predatory mortality is density-independent or density-dependent (solid line). The predation fraction of mortality p_i is varied (thin line: $p_i = 0.3$; intermediate line: $p_i = 0.6$; thick line: $p_i = 0.9$). The isoclines of the Lotka-Volterra competition model are shown for comparison (dotted line). (A) Model species when the mortality is density-independent. (B) Mimetic species when the mortality is density-independent. (C) Model species when the mortality is density-dependent. (D) Mimetic species when the mortality is density-dependent.

exceeds the benefit of protection. Traits for mimicry would cost the mimetic individuals, and also the benefit of mimicry negatively depends on their frequency (Ohsaki, 1995; Pfennig *et al.*, 2001). It is crucial to explore the balance between the benefit and cost for the model and mimic, incorporating the effects on population dynamics. Our model indicates that even if mimicry reduces predation of the mimic, it does not guarantee that the mimic spreads into allopatry of the model. The present results show that the benefit of mimicry for the mimic and the detriment of mimicry for the model need to be separately and explicitly investigated.

Where there is no resource competition between the model and mimetic species ($\alpha_{ij} = 0$; Fig. 6), our model predicts the equilibria analogous to those of Yamauchi (1993). Here intraspecific density dependence is assumed in each of the model and mimic species, such that each population goes to the carrying capacity. In this case, the model may be either reduced in density or eliminated as the result of additional predatory mortality.

The present model assumes that the mortality is equal to the frequency of mimetic individuals in the assemblage of the two species (equation 5). However, avian predators use the searching image to prey. They learn the searching image of palatable prey depending on frequency of encounter. Their learning efficiency may increase non-linearly with the relative frequency of the mimic (Rausher, 1978; Yamauchi, 1993). In that case, the predatory mortality (d) may change non-linearly with the mimic frequency. Whether it is linear or not, however, does not change the fundamental dependence of predatory mortality on the relative frequency of the mimetic individuals. Thus, the primary points of dynamic equilibria predicted by our model remain with no critical changes even if the predatory mortality increases non-linearly. The non-linearity in phase planes is already included because of frequency dependence in equation (5) (Yoshimura and Clark, 1994).

Batesian mimicry involves the reduction of mortality through avoidance of preying on the model species by an avian predator. Therefore, the adaptive evolutionary process of mimicry involves population dynamics in its essence. This paper provides theoretical analyses of population dynamics of Batesian mimicry under interspecific competition. The current results demonstrate the dependence of evolutionary processes of mimicry on the balance between the benefit and cost for the mimic and model species. Mimicry may be difficult to evolve when the cost to the model is large, because the model can be excluded depending on the initial condition (Fig. 2C). In contrast, mimicry is shown to occur when the benefit of the mimic is large, as the mimic can stably co-exist with the model (Fig. 2B). The present approach may also be useful for the population dynamic analysis of Müllerian mimicry, where both species gain the benefit of mimicry (Speed, 2001; Sasaki *et al.*, 2002; Franks and Noble, 2004).

ACKNOWLEDGEMENTS

We thank Steve Ellner for critical comments and helpful suggestions on the manuscript. This research was partly supported by grants-in-aid from the Ministry of Culture and Science in Japan to Takahiro Asami (grant #16405008) and Jin Yoshimura (grant #15570016).

REFERENCES

Bates, H.W. 1862. Contributions to an insect fauna of the Amazon valley. Lepidoptera: Heliconidae. *Trans. Linn. Soc. Lond.*, **23**: 495–566.

DeVries, P.J. 2002. Differential wing toughness in distasteful and palatable butterflies: direct evidence supports unpalatable theory 1. *Biotropica*, **34**: 176–181.

Emlen, J.M. 1968. Batesian mimicry: a preliminary theoretical investigation of quantitative aspects. *Am. Nat*, **102**: 235–241.

Estabrook, G.F. and Jesperson, D.C. 1974. Strategy for a predator encountering a model–mimic system. *Am. Nat*, **108**: 443–457.

Fisher, R.A. 1930. *The Genetical Theory of Natural Selection*. Oxford: Clarendon Press.

Ford, E.B. 1975. *Ecological Genetics*, 4th edn. London: Chapman & Hall.

Franks, D.W. and Noble, J. 2004. Batesian mimics influence mimicry ring evolution. *Proc. R. Soc. Lond. B*, **271**: 191–196.

Howarth, B., Edmunds, M. and Gilbert, F. 2004. Does the abundance of hoverfly (Syrphidae) mimics depend on the numbers of their hymenopteran models? *Evolution*, **58**: 367–375.

Huheey, J.E. 1964. Studies of warning coloration and mimicry: a mathematical model of model–mimic frequencies. *Ecology*, **45**: 185–188.

Johnstone, R.A. 2002. The evolution of inaccurate mimics. *Nature*, **418**: 524–526.

Kokko, H., Mappes, J. and Lindstrom, L. 2003. Alternative prey can change model–mimic dynamics between parasitism and mutualism. *Ecol. Lett.*, **6**: 1068–1076.

Luedeman, J.K., McMorris, F.R. and Warner D.D. 1981. Predators encountering a model–mimic system with alternative prey. *Am. Nat.*, **117**: 1040–1048.

Ohsaki, N. 1995. Preferential predation of female butterflies and the evolution of Batesian mimicry. *Nature*, **378**: 173–175.

Pfennig, D.W., Harcombe, W.R. and Pfennig, K.S. 2001. Frequency-dependent Batesian mimicry. *Nature*, **410**: 323.

Rausher, M.D. 1978. Search image for leaf shape in a butterfly. *Science*, **200**: 1071–1073.

Sasaki, A., Kawaguchi, I. and Yoshimori, A. 2002. Spatial mosaic and interfacial dynamics in a Müllerian mimicry system. *Theor. Pop. Biol.*, **61**: 49–71.

Sheppard, P.M. 1958. *Natural Selection and Heredity*. London: Hutchinson.

Sherratt, T.N. 2002. The evolution of imperfect mimicry. *Behav. Ecol.*, **13**: 821–826.

Sherratt, T.N. 2003. State-dependent risk-taking by predators in systems with defended prey. *Oikos*, **103**: 93–100.

Sherratt, T.N., Speed, M.P. and Ruxton, G.D. 2004. Natural selection on unpalatable species imposed by state-dependent foraging behaviour. *J. Theor. Biol.*, **228**: 217–226.

Speed, M.P. 2001. Batesian, quasi-Batesian or Müllerian mimicry? Theory and data in mimicry research. *Evol. Ecol.*, **13**: 755–776.

Speed, M.P. and Turner, J.R.G. 1999. Learning and memory in mimicry: II. Do we understand the mimicry spectrum? *Biol. J. Linn. Soc.*, **67**: 281–312.

Turner, J.R.G. 1977. Butterfly mimicry: the genetical evolution of an adaptation. *Evol. Biol.*, **10**: 163–206.

Turner, J.R.G. and Speed, M.P. 1996. Learning and memory in mimicry. I. Simulations of laboratory experiments. *Phil. Trans. R. Soc. Lond. B*, **351**: 1157–1170.

Turner, J.R.G., Kearney, E.P. and Exton, L.S. 1984. Mimicry and the Monte Carlo predator: the palatability spectrum and the origins of mimicry. *Biol. J. Linn. Soc.*, **23**: 247–268.

Wickler, W. 1968. *Mimicry in Plants and Animals*. New York: McGraw-Hill (English translation; 1974 reprint).

Yamauchi, A. 1993. A population dynamic model of Batesian mimicry. *Res. Pop. Ecol.*, **35**: 295–315.

Yoshimura, J. and Clark C.W. 1994. Population dynamics of sexual and resource competition. *Theor. Pop. Biol.*, **45**: 121–131.

APPENDIX 1

Let p_1** and p_2** be the threshold values of the predatory portions of mortality p_1 and p_2 respectively. These values are given by

$$p_1^{**} = \frac{b_{10} - m_{10} - (b_{10} - m_{10})\alpha_{12}}{m_{10}}$$

$$p_2^{**} = \frac{-b_{20} + m_{20} + (b_{20} - m_{20})\alpha_{21}}{m_{20}}$$

When $0 < p_i < p_i^{**}$, its nullcline curves downward. When $p_i = p_i^{**}$, it becomes a straight line. When $p_i > p_i^{**}$, it curves upward. Because of these curvature shifts, some phase planes become qualitatively different from the standard Lotka-Volterra model when $p_i < p_i^{**}$. The conditions of existence of these threshold values are derived from the range of p_i $(0 \le p_i \le 1)$ as

$$\frac{b_{10} - 2m_{10}}{b_{10} - m_{10}} \le \alpha_{12} \le 1$$

for p_1** and

$$1 \le \alpha_{21} \le \frac{b_{20}}{b_{20} - m_{20}}$$

for p_2**.

APPENDIX 2

The N_1- and N_2-intercepts, c_1 and c_2, for the model with density-independent mortality are

$$c_1 = \frac{b_{10} - (1 + p_1)m_{10}}{b_{10} - m_{10}} \frac{K_1}{\alpha_{12}}$$

and

$$c_2 = \frac{b_{20} - (1 - p_2)m_{20}}{b_{20} - m_{20}} \frac{K_2}{\alpha_{21}}$$

respectively. Their corresponding thresholds p_1* and p_2* are

$$p_1^{*} = \frac{(b_{10} - m_{10})(K_1 - \alpha_{12}K_2)}{m_{10}K_1}$$

$$p_2^{*} = \frac{(b_{20} - m_{20})(\alpha_{21}K_1 - K_2)}{m_{20}K_2}$$

For the density-dependent case, c_1 and c_2 are

$$c_1 = \frac{b_{10} - m_{10}}{p_1 b_{1k} + b_{10} - (1 + p_1) m_{10}} \frac{K_1}{\alpha_{12}}$$

$$c_2 = \frac{b_{20} - m_{20}}{-p_2 b_{2k} + b_{20} - (1 - p_2) m_{20}} \frac{K_2}{\alpha_{21}}$$

Their corresponding thresholds p_1* and p_2* are

$$p_1{}^* = \frac{(b_{10} - m_{10})(K_1 - \alpha_{12} K_2)}{(b_{1k} - m_{10}) \alpha_{12} K_2}$$

$$p_2{}^* = \frac{(b_{20} - m_{20})(\alpha_{21} K_1 - K_2)}{(b_{2k} - m_{20}) \alpha_{21} K_1}$$